Frontiers of Information Technology & Electronic Engineering
www.jzus.zju.edu.cn; engineering.cae.cn; www.springerlink.com
ISSN 2095-9184 (print); ISSN 2095-9230 (online)
E-mail: jzus@zju.edu.cn

Correspondence:

A high-precision terahertz retrodirective antenna array with navigation signal at a different frequency*

Zhong-bo ZHU[1,2], Wei-dong HU[†‡1], Tao QIN[3], Sheng LI[2], Xiao-jun LI[2],
Jiang-jie ZENG[3], Xian-qi LIN[3], Leo P. LIGTHART[1]

[1]*Beijing Key Laboratory of Millimeter Wave and Terahertz Technology, Beijing Institute of Technology, Beijing 100081, China*
[2]*National Key Laboratory of Science and Technology on Space Microwave, China Academy of Space Technology, Xi'an 710100, China*
[3]*School of Electronic Science and Engineering, University of Electronic Science and Technology of China, Chengdu 611731, China*
[†]E-mail: hoowind@bit.edu.cn

Received Oct. 24, 2019; Revision accepted Feb. 17, 2020; Crosschecked Mar. 3, 2020

Abstract: Future communications will provide higher transmission rates and higher operating frequencies. In addition, agile beam tracking will be an inevitable trend in technology development. The terahertz retrodirective antenna array proposed and discussed in this paper can be a better solution for agile beam tracking. The array receives a 40-GHz navigation signal and accurately retransmits a 120-GHz beam in the direction of the arrival wave. Simulation results indicate that the proposed array with a stacked sandwich structure has realized the tracking of the received wave. The scanning radiation pattern shows that the array gain is 23.87 dB at 19.9° when the incident angle is 20° with a relative error of only 0.5%, meaning that there is a lateral error of only 8.7 m at a transmission distance of 5 km.

Key words: Terahertz; Retrodirective antenna array; Terahertz communications; Conjugate mixing
https://doi.org/10.1631/FITEE.1900581 **CLC number:** TN821

1 Introduction

The terahertz wave is an electromagnetic wave with a frequency between 0.1 and 10 THz and a wavelength of 30–3000 μm. The spectrum is between the microwave and far-infrared, adjacent to the millimeter wave in its low-frequency segment, and adjacent to infrared in its high-frequency segment. As a new frequency band, terahertz has not been fully developed. Terahertz communication has the advantages of rich spectrum resources and high transmission rate. It is part of a broadband wireless access communication technology (Tb/s class) with great advantages for future mobile communication. Rosenworcel (2018) said at the Mobile World Congress that 6G can use the terahertz (THz) based network and spatial multiplexing.

However, terahertz communication is limited by radiated power and channel fading, making it impossible to achieve wide beam coverage. Adjusting the beam to point in coverage mode will be the best choice depending on the communication node requirements. In the case of high-speed motion of the node, narrow beam capture and tracking will become the key technology that needs to be addressed first. Currently, there are two technical approaches for beam adaptive acquisition and tracking of terahertz communication, i.e., traditional beam direction angle

‡ Corresponding author
* Project supported by the National Key R&D Program of China (No. 2018YFB1801505), and the National Natural Science Foundation of China (Nos. 61527805 and 61731001)
ORCID: Zhong-bo ZHU, https://orcid.org/0000-0003-1505-4880; Wei-dong HU, https://orcid.org/0000-0002-6051-3962

measurement tracking and novel beam retrodirective communication. The beam retrodirective communication can complete alignment communication through beam retrodirective without detecting the direction angle of the beam from the other party of the mobile communication system, and has a simple technical structure and a quick response (van Atta, 1959; Kokel, 2014; Roh et al., 2014).

The retrodirective antenna array has received much attention for satellite communication and mobile communication in recent years on account of its adaptive tracking properties (Hannan et al., 2017). The retrodirective antenna array can automatically retransmit a beam of echoes in the direction of the arrived signal with no need for any prior knowledge of the source location or extra complex digital signal processing units (Chen et al., 2010). The retrodirective array in Jacobs (1982) can approximate phase conjugation, but it is not applied to wireless communication and power transmission systems. This restricts its application. However, the retrodirective array is applied in short-range wireless power transmission (Leong et al., 2003b; Li and Jandhyala, 2012), and realizes channel adaptive tracking. In addition, the retrodirective array has the prospect of very broad application in 5G communications (Outerelo et al., 2015). With the increase of the operating frequency, it can be applied in the ultra-large-scale multiple-input multiple-output (MIMO) antenna arrays for 6G. Currently, some studies are focusing on the microwave band (Leong et al., 2003a). However, there are few focusing on terahertz retrodirective tracking applications.

In this paper, we present an innovative stacked sandwich structure to integrate eight channels of receiving and transmitting links into one whole cavity. This stacked sandwich increases channel consistency and miniaturizes the size of the retrodirective antenna array. The structure is easy to fabricate and can be easily integrated with antennas, mixers, multipliers, and amplifiers.

2 Retrodirective antenna array theory

2.1 Beam retrodirective theory

Consider an antenna array with a uniform linear array (Fig. 1). Assume that the radiated field is of a normalized amplitude, and the first array element on the left is the reference node. The far-field electric field distribution is (Samuel, 1990; Balanis, 2016)

$$E=\sum_{n=0}^{N-1}\mathrm{e}^{\mathrm{j}n\psi}=\frac{\sin(N\psi/2)}{\sin(\psi/2)}, \tag{1}$$

where ψ is the leading phase difference of the next array element relative to the previous one and N is the number of antenna elements. Assume that the array element spacing is d_1, the electromagnetic wavelength is λ_1, the added phase of conjugate mixing is σ, and the antenna radiation direction is β. Then the expression of ψ is

$$\psi=\frac{d_1 2\pi\cos\beta}{\lambda_1}+\sigma. \tag{2}$$

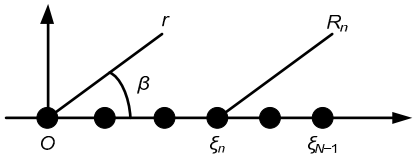

Fig. 1 Uniform linear array antenna

The Ka-band antenna array works in the receiving mode with an incident angle of α, and the antenna phase of each array element relative to the left is expressed as follows:

$$\theta=\frac{d_1 2\pi\cos\alpha}{\lambda_2}, \tag{3}$$

where λ_2 is the wavelength of the Ka-band signal. After phase conjugation, the leading phase difference becomes $-\theta$, and after triple frequency it is

$$\sigma=-3\theta=-\frac{3d_1 2\pi\cos\alpha}{\lambda_2}. \tag{4}$$

It is clear that the condition for retrodirection is $\alpha=\beta$. Setting $\psi=0$ for the maximum power radiation direction and substituting Eq. (4) into Eq. (2), the condition for retrodirection will be as follows:

$$\lambda_2=3\lambda_1 \text{ or } f_1=3f_2. \tag{5}$$

This is just a matched triple frequency condition, and the spaces between the array antenna elements are the

same. Therefore, it can be said that retrodirective antennas of different frequencies are feasible.

2.2 Phase transfer relationship

We present a block diagram for receiving and transmitting links in a single channel (Fig. 2). The signal received from ANT1 will be transmitted to MIX1, where LO1 is a higher local oscillator. In this condition, the mixer named MIX1 works as a conjugate mixer, which will ensure that the intermediate-frequency (IF) signal traveling on line *b* has a phase conjugated to its original phase.

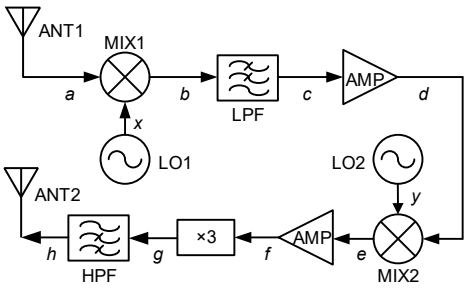

Fig. 2 Block diagram of receiving and transmitting links in a single channel

Reprinted from Zhu et al. (2019), Copyright 2019, with permission from IEEE

The distances between elements of the retrodirective antenna array are the same in the cases of 40 GHz and 120 GHz, but the phase of the signal radiated from ANT2 is three times that of the signal received from ANT1 with a conjugated relationship. The directions of the two signals will be exactly reversed.

Under this logic, if all channels of the antenna array play the same role, a pilot signal with a 40-GHz frequency is received, and a 120-GHz reverse signal with information modulated on it will be transmitted to the pilot end point. The sub-terahertz retrodirective antenna array can be used to set up a satellite communication link with the function of satellite tracking.

3 Retrodirective antenna array design

3.1 Structural design

To achieve channel integration, we propose a stacked sandwich structure. Fig. 3 shows the details of the stacked sandwich (Zhu et al., 2019). As one of the eight-channel links, all circuits are fabricated on the substrate Rogers RT/duroid 5880 (ε_r=2.2, $\tan\delta$= 0.0009, thickness=0.508 mm) as the middle layer of the sandwich, while the upper and lower metal cavities are separately processed and assembled with the substrate.

As shown in Fig. 3, the pilot signal receiving antenna at the low-frequency side of the retrodirective antenna array is designed as a wide-side slotted antenna. A microstrip-SIW (substrate integrated waveguide)-antipodal finline transition structure was adopted (Hao et al., 2005). Then there are a downconverter and a low-pass filter, followed by an amplifier. The DC and local oscillator are designed for the other side of the array. This gives convenient power supply placement and source feeding.

To minimize the antenna array, the high-frequency link circuit is designed along with the low-frequency chain. It is the mirror of the low-frequency signal chain, with the high-frequency chain composition by the sequence upconverter, amplifier, tripler, microstrip-SIW-RW (rectangular waveguide) transition, high-pass filter, and H-plane horn antenna.

3.2 Design of a 120-GHz transmit antenna array

The 120-GHz antenna element is designed as shown in Fig. 4a. The H-face open horn antenna is adopted, and has a microstrip interface. The horn has a rectangle aperture of 10 mm×2 mm and a gradual length of 30 mm. Therefore, the 120-GHz antenna array is divided into three steps: microstrip line transition, antenna element, and antenna array. From the simulation shown in Fig. 4b, we can see that S11 is below −15 dB and S12 is better than −0.38 dB from 116 to 124 GHz, with a bandwidth of transition structure of 8 GHz.

In the design of the terahertz radiating element, the radiation pattern of the antenna unit will also be considered. The radiation space is constructed by the simulation software environment, and the transmission transition circuit is combined with the antenna radiating element into the radiation environment. The excitation source is set at the entrance port of the transmission transition circuit. This can lead to the radiation pattern of the antenna unit (Fig. 5).

It can be seen from the simulation results that the terahertz radiating element has a significant enhancement on the realized gain. With the maximum

gain being 15 dBi, the levels of cross-polarization in both the E-plane and H-plane are relatively low (Fig. 5). This result is in good agreement with the structure of the antenna unit. It can also be seen from the 3D pattern that the grating flap suppression effect at other angles is better, and there is no sudden high gain grating flap.

3.3 Design of a 40-GHz band receiving antenna array

The pilot signal receiving antenna of the beam retrodirective antenna is a 40-GHz band antenna array. To be well integrated with the terahertz radiating antenna array, the 40-GHz antenna adopts a gradient slotted antenna with an SIW upper and lower metal surface gradient. The antenna in this structure has low profile, with a light and thin structure.

The receiving antenna in the retrodirective antenna array designed here adopts the finline gradient slotted antenna form, which is formally based on the above considerations (Fig. 6). However, the quasi-planar structure superior to the finline makes it difficult to directly connect with the integrated circuit.

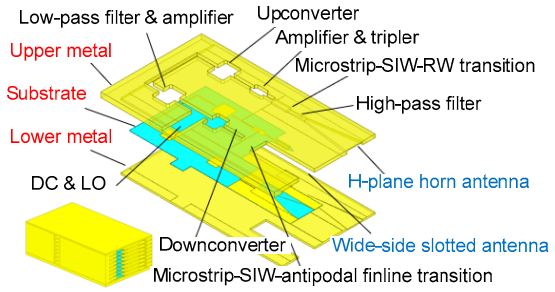

Fig. 3 Sketch of the proposed stacked sandwich structure and stacked sandwich in a single channel in details for a 120-GHz received antenna array

Reprinted from Zhu et al. (2019), Copyright 2019, with permission from IEEE

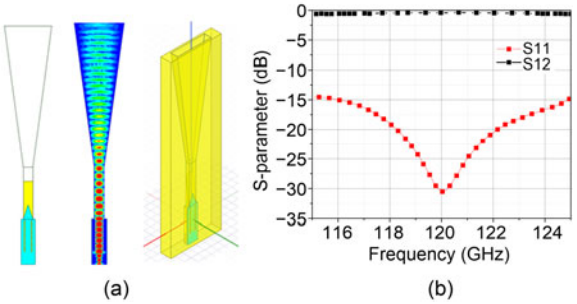

Fig. 4 The 120-GHz horn antenna and transition circuit schematic (a) and their simulation results (b)

Therefore, a finline-to-SIW transition is adopted in this scheme, and the probe-to-waveguide transition structure is adopted at the SIW end to realize the entire feeder network connection. In addition, if the antenna end is directly connected to the millimeter wave chip by bonding gold wire, the microstrip line can be used at the end of the SIW.

Fig. 7 shows the simulation results of the structure and return loss of the 40-GHz band receiving antenna array. Since the bandwidth of the pilot signal itself is very narrow, in the communication system, the pilot signal provides mainly the direction identification and the signal itself does not load the broadband communication information. Part of the circuit design can pay more attention to the narrowband characteristic indicators. The retrodirective antenna array designed in this study is for mobile communication in fast motion. Considering the influence of phenomena such as the Doppler effect, the system design bandwidth is 300 MHz. When the

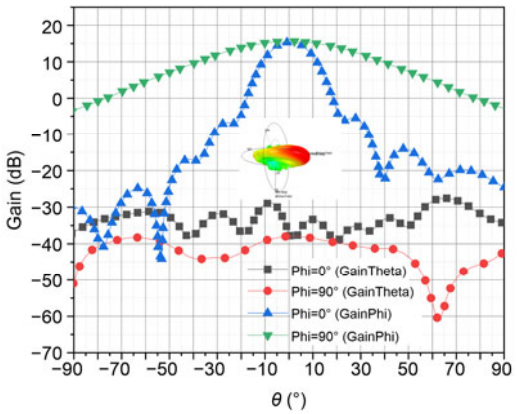

Fig. 5 Two- and three-dimensional patterns of the terahertz antenna element under simulation software

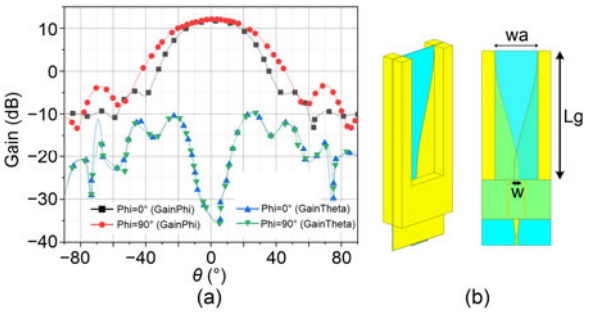

Fig. 6 Simulation result (a) and stacked sandwich in a single channel (b) for a 40-GHz receiving antenna array

(b) is reprinted from Zhu et al. (2019), Copyright 2019, with permission from IEEE

retrodirective signal is generated, the Doppler shift is compensated for in the baseband circuit.

Because of the low frequency of the receiving antenna in the 40-GHz band and the relatively uncomplicated circuit structure, the transition circuit and the antenna are co-simulated in this part of the design. Figs. 8a and 8b show the scanning 0°-pattern and active reflection, respectively. Figs. 9a and 9b are the scanning 10°-pattern and the active reflection, respectively. It can be seen from Figs. 8a and 9a that, because of mutual coupling, the pattern of each antenna unit is different. The gain of the edge antenna is 10 dB, but the gain of the central unit is only about 8.5 dB. This distribution will cause the sidelobe level of the array pattern to rise and the pattern to be worse. At the same time, because the unit pattern is different, and each channel receives the navigation signal, the energy will be inconsistent, which will eventually affect the transmit beam. However, if the beam pointing deviation is fully reflected in the phase change, a phase change of 1.5° will result in a fixed 3.8° phase difference between the Ka-band antenna elements. This phase difference will be tripled in the 120-GHz antenna array, resulting in a phase difference of 11.3°. We bring this phase difference into the 120-GHz antenna and compare it to the ideal antenna pointing. It can be observed that the actual beam pointing of the 120-GHz array deviates by 1°–2° after a deviation of 11.3°. Since the 120-GHz array has a beam width of 6° and a beam coverage of 5 m, theoretically this deviation will not affect the acceptance criteria.

4 System simulation results

In the simulation of channels, the receiving antenna array receives incident plane wave excitation; therefore, the receiving phase formed on each element of the array is recorded. Because of the phase conjugation processing of the downconverter (Li and Jandhyala, 2012), the phase gradient of each channel should be reversed. After the signal passes through the tripler, the phase of each channel is tripled, meaning that the phase difference between the channels is also tripled.

Other devices in the channel add only phase shifts to the signal, but the additional phase shifts for all channels are equal. The beam direction of the transmitting antenna array depends on the phase difference between the elements, independent of the value of the phase, so the additional phase shifts of other devices do not affect the beam pointing. Fig. 10 shows the scanning radiation pattern of the retrodirective array versus different incident angles. It can be seen that the echo beam pointing is very close to that of the arriving signal. When the incident angle is 20°, the retrodirective array automatically forms a beam pointing at 19.9° with a relative error of only 0.5%, meaning that there is a lateral error of only 8.7 m at a transmission distance of 5 km. Array scanning gains are 23.10, 21.48, 22.68, 23.70, and 23.87 dB at the angles of 0.0°, 4.6°, 10.2°, 15.0°, and 19.9°, respectively.

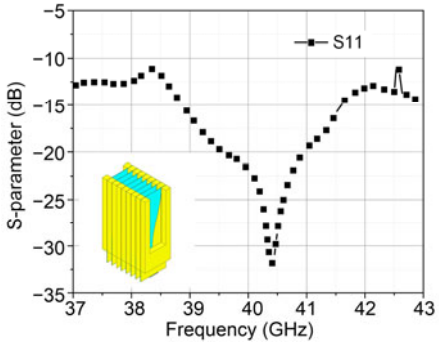

Fig. 7 The 40-GHz receiving antenna array integrated structure and the return loss of its circuit

5 System test results

In this solution, the core parameter is the phase, and the operation of the system depends on whether the phase after multi-stage mixing and multiplying maintains linear transmission. To verify this condition, a test scheme (Fig. 11) was constructed. Because a higher frequency of the feed signal can reflect the change of phase, the test scheme did not use a 40-GHz feed, but chose 120 GHz as the pilot signal to feed into the system.

In this test scenario, the phase relationship was measured using an agilent vector network analyzer (E8363C). The appropriate network analyzer port 1 was used as the transmitting port of the signal. The transmitting signal was radiated by the 120-GHz horn antenna. Both the transmitting and receiving antennas

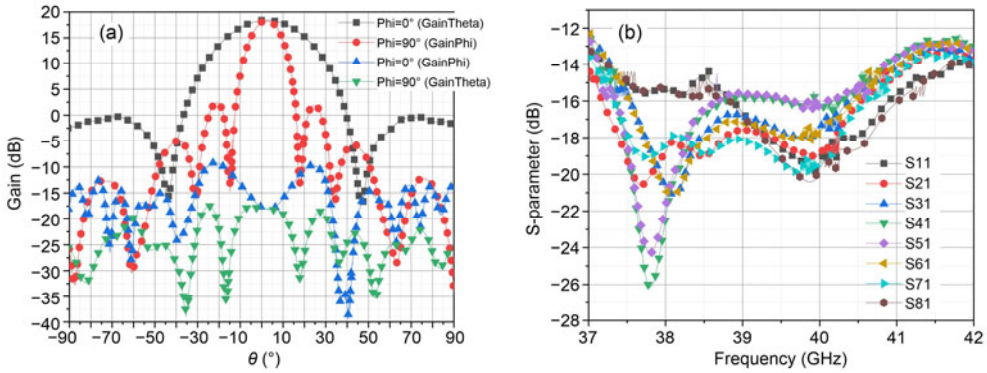

Fig. 8 Scanning 0°-pattern of the 40-GHz band antenna array (a) and the active reflection of the 40-GHz band antenna array when scanning at 0° (b)

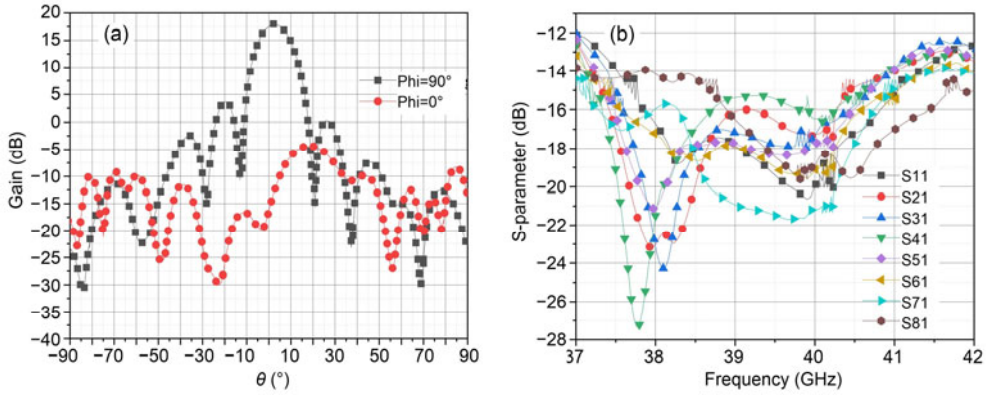

Fig. 9 Scanning 10°-pattern of the 40-GHz band antenna array (a) and the active reflection of the 40-GHz band antenna array when scanning at 10° (b)

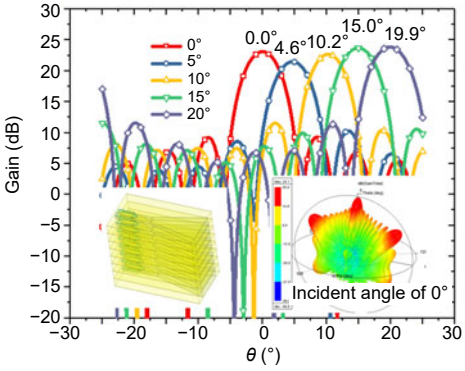

Fig. 10 Scanning radiation pattern of the retrodirective array versus different incident angles

Reprinted from Zhu et al. (2019), Copyright 2019, with permission from IEEE

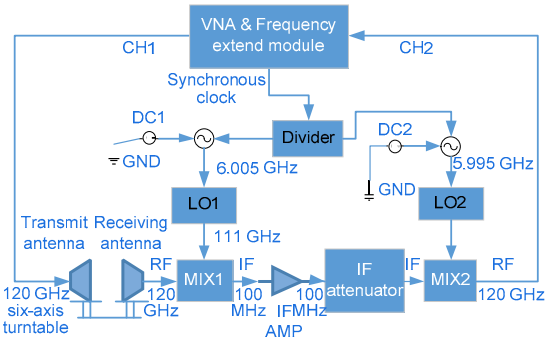

Fig. 11 Block diagram of the phase transfer relationship verification system

were placed on the six-axis turntable. This is convenient for distance adjustment and for high and low adjustment. After receiving the signal, the receiving antenna first received the signal. After that, conjugate mixing was completed by the downconverter (MIX1), the output intermediate frequency signal was fed into the upconverter after being adjusted by the intermediate frequency amplifier (IF AMP) and the attenuator (IF attenuator), and the local oscillators (LO1 and LO2) of the two inverters were synchronized by the clock of the vector network analyzer backplane. In this case, the phase synchronization between the vector network analyzer and the local oscillator can

be maintained without introducing random phase interference. The test scenario and results of the phase relationship are shown in Fig. 12.

It can be seen that the phase decreased linearly with the increase of the frequency, which is consistent with the theory, and the phase slope changed when the distance was extended. This proves that the test satisfies the acceptance criteria in the passive case.

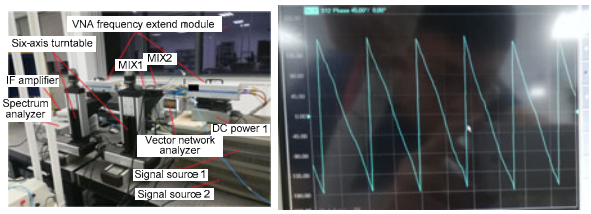

(a) (b)

Fig. 12 Phase relationship actual test scene graph (a) and phase relationship actual result (b)

6 Conclusions

The retrodirective array for terahertz tracking has been designed and verified in simulations in this paper. Based on the retrodirective array theory, this array has been developed and received a 40-GHz navigation signal and retransmitted a 120-GHz beam in the direction of the arrival wave. Simulation results indicated that the proposed array with the stacked sandwich structure can realize the tracking of the arrival wave. The scanning radiation pattern showed that the array gain is 23.87 dB at 19.9° when the incident angle is 20° with a relative error of only 0.5%, meaning that there is a lateral error of only 8.7 m at a transmission distance of 5 km. The findings are significant for tracking of terahertz satellite communication systems, which lays the foundation for future work. In the future, this array will be combined with communication links, to achieve not only tracking, but also data transmission and high-speed communication functions.

Contributors

Zhong-bo ZHU designed the research and drafted the manuscript. Xiao-jun LI helped on communication antenna request greatly, Wei-dong HU helped optimize the simulation model, Leo P. LIGTHART gave a lot of theoretical guidance, and Xian-qi LIN helped optimize the antenna circuit. Tao QIN, Jiang-jie ZENG, and Sheng LI processed the data. Xian-qi LIN and Wei-dong HU helped organize the manuscript. Zhong-bo ZHU and Wei-dong HU revised and finalized the manuscript.

Compliance with ethics guidelines

Zhong-bo ZHU, Wei-dong HU, Tao QIN, Sheng LI, Xiao-jun LI, Jiang-jie ZENG, Xian-qi LIN, and Leo P. LIGTHART declare that they have no conflict of interest.

References

Balanis CA, 2016. Antenna Theory: Analysis and Design. John Wiley & Sons, Hoboken, USA.

Chen L, Wang XH, Shi XW, et al., 2010. Design of a broadband frequency offset Van Atta array. *PIER Lett*, 13:161-171. https://doi.org/10.2528/PIERL10020507

Hannan A, Hasan A, Tarar MA, 2017. Simplified design, simulation, and lab-environment measurement scheme for retro-directive antenna arrays. *Microw Opt Technol Lett*, 29:2890-2893. https://doi.org/10.1002/mop.30849

Hao ZC, Hong W, Chen JX, et al., 2005. Compact super-wide bandpass substrate integrated waveguide (SIW) filters. *IEEE Trans Microw Theory Techn*, 53(9):2968-2977. https://doi.org/10.1109/TMTT.2005.854232

Jacobs SF, 1982. Experiments with retrodirective arrays. *Opt Eng*, 21(2):212281. https://doi.org/10.1117/12.7972895

Kokel SJ, 2014. Retrodirective Phase-lock Loop Controlled Phased Array Antenna for a Solar Power Satellite System. PhD Thesis, Texas A&M University, Texas, USA.

Leong KMKH, Miyamoto RY, Itoh T, 2003a. Moving forward in retrodirective antenna arrays. *IEEE Potent*, 22(3):16-21. https://doi.org/10.1109/MP.2003.1232308

Leong KMKH, Miyamoto RY, Itoh T, 2003b. Ongoing Retrodirective Array Research at UCLA. Technical Report SPS2002-08, University of California, Los Angeles, USA.

Li Y, Jandhyala V, 2012. Design of retrodirective antenna arrays for short-range wireless power transmission. *IEEE Trans Antenn Propag*, 60(1):206-211. https://doi.org/10.1109/TAP.2011.2167897

Outerelo DA, Alejos AV, Sanchez MG, et al., 2015. Microstrip antenna for 5G broadband communications: overview of design issues. Proc IEEE Int Symp on Antennas & Propagation & USNC/URSI National Radio Science Meeting, p.2443-2444. https://doi.org/10.1109/APS.2015.7305610

Roh W, Seol JY, Park J, et al., 2014. Millimeter-wave beamforming as an enabling technology for 5G cellular communications: theoretical feasibility and prototype results. *IEEE Commun Mag*, 52(2):106-113. https://doi.org/10.1109/MCOM.2014.6736750

Rosenworcel J, 2018. Remarks of Commissioner Jessica Rosenworcel Mobile World Congress Americas, Los Angeles, California, September 13, 2018.

Samuel YL, 1990. Microwave Devices and Circuits. Prentice Hall, Englewood.

van Atta LG, 1959. Electromagnetic Reflector. US Patent, 2 908 002.

Zhu ZB, Hu WD, Lin XQ, et al., 2019. A sub-terahertz retrodirective antenna array for satellite tracking. Proc 44th Int Conf on Infrared, Millimeter, and Terahertz Waves, p.1-2. https://doi.org/10.1109/IRMMW-THz.2019.8873909